



Dr. Muna K. Abbass

Dept. of production Engineering and  
Metallurgy, University of Technology  
Email:mukeab2005@yahoo.com

## Effect of Rare Earth Oxides ( $Y_2O_3$ , $Nd_2O_3$ ) on Oxidation Kinetics of Al-Li base alloy

Muna K. Abbas; Assist Prof.

### Abstract:

*The oxidation of Al-Li base alloy containing small amounts of rare earth (RE) oxides such as  $Y_2O_3$  and  $Nd_2O_3$  particles has been studied at temperatures between 300°C and 550°C. The lithium is selectively oxidized in Al-Li alloys and the parabolic rate constants for the growth of the resulting oxides layer  $Li_2O$ ,  $LiAl_5O_8$ ,  $Li_2CO_3$  and  $Li_5AlO_4$  are about an order of magnitude higher than those for growth of oxides on alloy (Al-Li) with RE oxides. Alloys used in this study were prepared by melting and casting in a permanent steel mould under controlled atmosphere.*

*It was found that 0.2% $Y_2O_3$  containing alloys possess the lowest oxidation rate and show great improvements in oxidation resistance compared to the base alloy.*

*Oxides found on base alloy are subjected to cracking and spalling during thermal shock at high temperature i.e. 500°C and 550°C. Identification of oxidation kinetics was carried out by using weight gain measurements while scanning electron microscopy (SEM) and x-ray diffraction analysis were used for microstructural morphologies and phase identification of the oxide scales. The weight gain measurement results suggest that the oxidation kinetic of all studied alloys follows the parabolic law in most experimental tests under the different temperatures except at 300°C oxidation kinetic follows almost a logarithmic rate law.*

**Keywords:** Material, metal.

### 1. Introduction.

Al-Li alloys offer attractive combination of properties for an extensive use in aircraft structures, reducing the density and increasing other properties like stiffness, fatigue resistance. These properties could already lead structural weight reduction of up to 15% on commercial airliners [1-3]. However these alloys undergo severe oxidation at high temperatures approximately an order of magnitude higher than the Li-free Al-base alloys. This tendency creates serious problems during high temperatures processing such as solution heat treatment, homogenization, forming and aging [4-6].

Procedures for minimizing oxidation and lithium depletion during processing of Al-Li alloys are discussed elsewhere. Some workers Bakri et al, 1992[7] and Haidary et al, 2000 [8] also reported those trace element additions of (Y, Ge, Te) known to inhibit oxidation in certain Al-alloys. The rare earth element (REE) is now well known to improve the high temperature oxidation of stainless steel. Many authors have proposed theories about this beneficial effect [1-4]. The use of RE oxide coating has the advantage of not affecting adversely the mechanical properties of the alloy and it has also the potential of being used on surfaces of metallic components exposed to high temperature oxidizing environments [9,10] due to their excellent oxidation resistance and improve the resistance to scale spallation. The RE elements can be added to heat resistant alloys either in elemental form or as oxide dispersion [10, 11]. The RE can also be introduced into the surface by ion implantation

techniques or applied superficially by a variety of techniques.

In this research the RE oxides Nd<sub>2</sub>O<sub>3</sub> (0.2%) and Y<sub>2</sub>O<sub>3</sub> (0.2%) introduced into the base alloy (Al-Li-Cu-Mg) by a casting method using mechanical stirring to disperse Y<sub>2</sub>O<sub>3</sub> and Nd<sub>2</sub>O<sub>3</sub> particles in the molten base alloy and pouring the melt in steel molds. The present paper is concerned with the effect of RE oxides Nd<sub>2</sub>O<sub>3</sub> and Y<sub>2</sub>O<sub>3</sub> on the oxidation behavior and oxidation rate constant (K<sub>p</sub>) of a solution hardened alloy (8090) at temperatures (300-550)°C.

## 2. Experimental procedures

Alloys were prepared by melting and pouring the melt in a permanent steel mold under controlled atmosphere by passing argon gas through an orifice in

the cover of graphite crucible where the melting occurs and the RE oxides of Nd<sub>2</sub>O<sub>3</sub> and Y<sub>2</sub>O<sub>3</sub> (0.2wt% for each one) with size distribution of (3-10)µm were added and dispersed in matrix of base alloy A (Al-2.4% Li-1.2% Cu-1.0% Mg- 0.15%Zr), and obtained alloy B and C which contain 0.2% Nd<sub>2</sub>O<sub>3</sub> and 0.2% Y<sub>2</sub>O<sub>3</sub> respectively. The prepared alloys were homogenized in dry air at 530°C for 18hr followed by hot rolling up to 50% reduction. The solution heat treatment has been done at 530°C for an hour and water quenching then aging at 190°C for 10hr for all specimens. The chemical composition analysis of the base alloy A (Al-Li-Cu-Mg) was carried out by using spectral analysis device of spectrometer type ARL. Results of the analysis with the standard value for each element and density are shown in Table (1).

**Table (1):** Analysis chemical composition and density of the base alloy A (Al-Li-Cu-Mg)

Element (wt%)	Li	Cu	Mg	Zr	Ti	Fe	Si	Rem	ρ (g/cm <sup>3</sup> )
Measured value	2.4	1.2	1.0	0.15	0.03	0.03	0.03	Al	2.561
Standard value(8090)	2.2-2.7	1.0-1.4	0.6-1.1	0.04-0.16	0-0.10	0-0.30	0-0.2	Al	2.554

Oxidation specimens were cut from ingot after homogenization as discs in dimensions of 15mm diameter and (2-2.5)mm thickness. These specimens were grounded with water by using emery paper of SiC with different grits (220, 320, 500 and 1000). Polishing process was done by using diamond paste (grade 1µm) with special polishing cloth and lubricant. They were cleaned with water and alcohol and dried with hot air. The specimens were oxidized at temperature range of 300°C to 550°C in static air at atmospheric pressure in a vertical tube furnace with uniform hot zone. The temperature of the hot zone is controlled by thermocouple type K. The oxidation kinetics were determined by the weight gain method with a microbalance of an accuracy of 0.1mg, where the specimen was placed into the hot furnace after reaching the required temperature, each specimen was hung using Pt-wire.

Upon completion of the kinetic measurements the oxidized specimens were examined optically to evaluate their surfaces topography. Standard x-ray diffraction techniques were employed for phase identification of the alloy and the oxidation products, using Philips 1830 x-ray diffractometer with Cu.Kα radiation (1.547Å).

## 3-Results and Discussion

### 3-1 Microstructure of prepared alloys

All alloys were fabricated by a method of melt stirred composing and pouring the melt in steel mould. Figure (1) shows the microstructure of prepared alloys (A, B and C) after casting and deformation and solution heat treatment respectively. The micrographs of the base alloy A (Al-Li-Cu-Mg), alloy B and alloy C with the RE oxides Nd<sub>2</sub>O<sub>3</sub> and Y<sub>2</sub>O<sub>3</sub> particles uniformly distributed in the matrix of alloy.

### 3-2 Oxidation behavior of alloy (A)

Isothermal oxidation measurements revealed weight gain increases with time. At temperature 300°C, shown in Figure (2) indicates that the weight gain (ΔW/A) increases until reaching certain values, it becomes roughly constant value of (ΔW/A) at (60hr). This is due to formation of protective oxide layer of alumina (Al<sub>2</sub>O<sub>3</sub>) on a base alloy (Al-Li-Cu-Mg).

Previous studies [3, 4] with Al-Li base alloy have shown that during the initial period of oxidation both Li<sub>2</sub>O and Li<sub>2</sub>CO<sub>3</sub> are formed on the surfaces of specimen and as oxidation continues the oxide layers become continuous separating the Al<sub>2</sub>O<sub>3</sub> from the alloy. The variation of the shapes of the

weight gain change vs time curves for alloy A are also due to the increase amount of oxide layers that are formed on the surface of these specimens. Show Figures (3, 4, and 5).

The results obtained for alloy (A) show that the oxidation kinetic of this alloy is controlled by interdiffusion of lithium through  $\text{Al}_2\text{O}_3$  scale, and the oxide /gas interface reaction which involves the formation of different oxides  $\text{Li}_2\text{CO}_3$  scale,  $\gamma$ - $\text{LiAlO}_2$ ,  $\text{LiAl}_5\text{O}_8$  and  $\alpha$ - $\text{Li}_5\text{AlO}_4$  in addition to the  $\text{Al}_2\text{O}_3$  scale as shown in x-ray diffraction analysis ( see appendixes A & B ).

Data for oxidation of an alloy (A) (Al-Li-Cu-Mg) at  $550^\circ\text{C}$  are also included for comparison and it is obvious that the oxidation rate of alloy A in terms of weight gain is greater than that for RE-containing alloys at this temperature. Similar results were obtained at other temperatures within the interval of oxidation of (60hr).

The oxidation kinetics for alloy (A) obey a parabolic law (relationship) at the weight gain ( $\Delta W/A$ ) measurement. However such a oxidation rate law was approached for specimens oxidized at  $400^\circ\text{C}$ ,  $500^\circ\text{C}$  and  $550^\circ\text{C}$  after (60hr) of oxidation time.

### 3.3 Oxidation behavior of alloys (B, C)

Comparison of results obtained for the oxidation of an alloy (A) (Al-Li-Cu-Mg) to those alloys containing 0.2% $\text{Nd}_2\text{O}_3$  and 0.2% $\text{Y}_2\text{O}_3$  (alloy B and alloy C) respectively. It was found that dispersion of RE oxide in matrix of base alloy (Al-Li-Cu-Mg) improves the oxidation resistance and shown that the weight gain ( $\Delta W/A$ ) of alloy (C) was lower than that of other alloy (A) and alloy (B) at all oxidation temperatures as shown in Figures (2,3,4 and 5). This is due to the role of  $\text{Y}_2\text{O}_3$  particles in reducing oxidation rate in the base alloy (A) and decreasing growth rate of  $\text{Li}_2\text{O}$  scale and other oxide layers, show Fig(6). Since  $\text{Y}_2\text{O}_3$  atoms improved adhesion between scale and substrate alloy by two mechanisms [10,13]. The oxide scales formed on alloy (C) are also thinner than the scales that are formed on alloys with similar lithium content but which do not contain dispersed yttria ( $\text{Y}_2\text{O}_3$ ) particles. Oxidation behavior of alloy (B) was similar to alloy (C) at all temperatures ( $300$ - $550^\circ\text{C}$ ), show Figures(7 and 8).. X-ray analysis of the oxide scale on the alloy (B) and (C) indicated that  $\text{Nd}_2\text{O}_3$  and  $\text{Y}_2\text{O}_3$  respectively were always present in external scales. Since the external scales did not spall and crack significantly during thermal shock from high temperature  $550^\circ\text{C}$  and  $500^\circ\text{C}$  after oxidation time (50hr). In case of alloy (C), the oxide layer remains

sound and unaffected by thermal shock. This could be attributed to  $\text{Nd}_2\text{O}_3$  and  $\text{Y}_2\text{O}_3$  atoms effect in reducing vacancies at the oxide /metal interface and modify the diffusivity and solubility of alloying element in alloy [13,14].

The weight gain result for alloy (B) containing 0.2% $\text{Nd}_2\text{O}_3$  was greater than that of alloy (C) containing 0.2% $\text{Y}_2\text{O}_3$  for up to 60 hr of oxidation periods but less than that of alloy (A). This is due to the role of  $\text{Nd}_2\text{O}_3$  particles inhibit growth of oxide scales at high temperatures and improvements of oxides plasticity and adhesivity. These results agree with those of other workers Chevalier et al, 1998[14]

### 3.4 Effect of Thermal Shock

The effect of thermal shocks on the mechanical integrating of scale was studied. The specimens were subjected to thermal shock by quenching it rapidly from the oxidation temperature to room temperature and then was returned to furnace and the weight was recorded again, the loss in weight indicates scale breakdown (spalling), Oxides formed on alloy (A) crack and spall largely when subjected to thermal shock after 50hr of oxidation at  $550^\circ\text{C}$  as shown in Figure (9).

In case of alloy (B) ( $\text{Nd}_2\text{O}_3$ -containing alloy) the oxides also cracked and spalled during the thermal shock after 50hr of oxidation at  $550^\circ\text{C}$  but the effect of thermal shock was less severe than that of alloy A as shown in Figure(10).

In case of alloy (C) ( $\text{Y}_2\text{O}_3$ -containing alloy) the oxides layer remain sound and unaffected by thermal shocks as shown in Figure (11).

The spalling was not detected at lower temperature ( $300^\circ\text{C}$  and  $400^\circ\text{C}$ ). This could be explained by the fact that the oxide layer was more adhesion and protective compared to that produced at ( $500^\circ\text{C}$  and  $550^\circ\text{C}$ ). The RE oxides are also considered to act as preferential nucleation sites for  $\text{Al}_2\text{O}_3$  formation. Entrapment of RE oxides within  $\text{Al}_2\text{O}_3$  layer has been observed. The x-ray diffraction analysis showed that  $\text{Nd}_2\text{O}_3$ ,  $\text{Y}_2\text{O}_3$  particles were present in oxide scale on the alloy B and C respectively.

Proof of conclusion this has been observed and similar observations were presented by Papaioacovou and Hussey [15] for scale growth on ceria ( $\text{CeO}_2$ ) coated on Fe-Cr alloys.

### 3-5 Results of oxidation kinetics

Results of oxidation of base alloy (Al-Li) are given in terms of weight gain ( $\Delta W/A$ ) presented in kinetics curves, show Figures(2,3,4 and 5). Weight gains were recorded for kinetic of oxidation in dry

air at temperature range (300°C-550°C) for up to 60hrs.

For the parabolic oxidation kinetics, the rate equation takes from:

$(\Delta W/A) = Kt^{0.5}$	<b>1</b>
---------------------------	----------

A plot of square weight gain ( $\Delta W/A$ ) vs time (t) gives a line, the slope of which is the parabolic rate constant ( $K_p$ ) as the following equation:

$(\Delta W/A)^2 = K_p t$	<b>2</b>
--------------------------	----------

To give  $K_p$  in units ( $\text{mg}^2\cdot\text{cm}^{-4}\cdot\text{sec}^{-1}$ ). The  $K_p$  for three alloys (A, B and C) at temperatures 400°C, 500°C and 550°C are calculated and the liner lines represent the squares curves fitting as shown in Figures (12, 13 and 14). The parabolic oxidation rate constants ( $K_p$ ) for alloys are listed in Table (2). The oxidation kinetics for alloy(A), alloy (B) and alloy(C) obey a parabolic law (relationship) at the weight gain ( $\Delta W/A$ ) measurements, however such oxidation rate law was approached for specimens oxidized at 400°C, 500°C and 550°C after (60 hr) of oxidation time.

From experimental data plot of  $\text{Log } K_p$  vs ( $1/T$ ), an activation energy(Q) was calculated from least square fitting ( $R^2=0.98$ ) of the observed data in the temperatures range from 400°C to 550°C to be (169.86, 166.85, 168.44) KJ/mol for alloys(A, B, C) respectively as shown in Figure (15).

$K_p$  that obeys an Arrhenius - type equation of the following [16]:

$K_p = K_0 \exp(-Q/RT)$	<b>3</b>
-------------------------	----------

where  $K_p$  is the parabolic oxidation rate,  $K_0$  is the pre- exponential value,  $Q$  is the activation energy,  $T$  is the temperature and  $R$  is the universal gas constant

[8.33 (J/ K )/mol] or 1.987 cal /K /mol. A linear regression analysis of the equation (3) results in the following relationships for  $K_p$  as a function of temperature :

$K_p = 4 \cdot 10^7 \exp(-20392/T)$	<b>4</b>
-------------------------------------	----------

AlloyA

$K_p = 1 \cdot 10^7 \exp(-20031/T)$	<b>5</b>
-------------------------------------	----------

AlloyB

$K_p = 5 \cdot 10^6 \exp(-20222/T)$	<b>6</b>
-------------------------------------	----------

AlloyC

The weight gain ( $\Delta W/A$ ) data for each temperature test is plotted as shown in Figures (2,3, 4 and 5) as the evolution of the mass gain ( $\Delta W/A$ ) of the sample as a function of oxidation time. The initial kinetic is rapid but the rate of ( $\Delta W/A$ ) gradually decreases at longer times the kinetics can be described by examining the growth rate time constant or n-value which is found as the exponent in the following equation:

$(\Delta W/A) = K t^n$	<b>7</b>
------------------------	----------

$\text{Log}(\Delta W/A) = n \log t + C_1$	<b>8</b>
---	----------

The slop of a log-log plot gives the n-value, the growth rate time constant which provides an indication of the mechanism controlling oxidation and  $C_1$  is a constant represent the intersect point of the curve with y-axis as shown in Figures (16, 17 and 18)

At 500°C, the n-value is about 0.5, i.e. parabolic behavior is found. Another

n-values are shown in the Table (2). When the value of (n) is greater or lower than 0.5 then oxidation kinetic does not fall in the simple parabolic behavior and this implies faster or lower oxidation rate. For example, for  $n > 0.5$  it is an overparabolic, while for  $n < 0.5$  there is underparabolic (sub - parabolic)[17]. Results have shown that the subparabolic may be found because of grain boundary (short circuits) mechanism [18]. Deviation from theoretical value of  $n = 0.5$  can be explained by an oxide layer cracking, leading to a sudden increase of the surface area in contact with oxygen and thus to an acceleration of the oxidation kinetics.

Table (2): Values of n-value and  $K_p$

Alloy	Temperature °C	n- Values	Kp (mg <sup>2</sup> .cm <sup>-4</sup> .s <sup>-1</sup> )
Alloy A	300	--	---
	400	0.426	2.40E-06
	500	0.547	1.97E-04
	550	0.425	5.02E-04
Alloy B	300	--	---
	400	0.326	1.10E-06
	500	0.549	1.06E-04
	550	0.407	1.94E-04
Alloy C	300	--	---
	400	0.437	4.00E-07
	500	0.498	2.74E-05
	550	0.529	8.44E-05

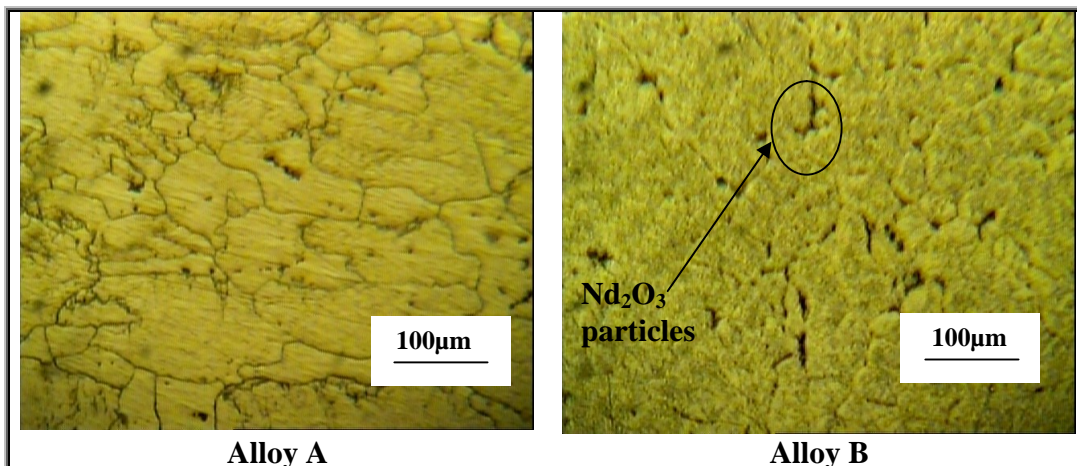
#### 4. Conclusions

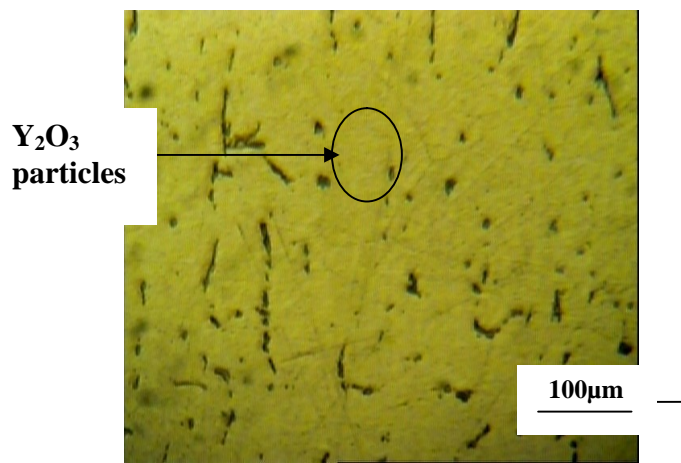
- 1-The oxidation kinetics for all investigated alloys did obey to the parabolic law at temperature 400°C, 500°C and 550°C except at 300°C oxidation kinetic follows almost a logarithmic law.
- 2-The oxidation rate constant (kp) for alloys containing RE oxides (Y<sub>2</sub>O<sub>3</sub> & Nd<sub>2</sub>O<sub>3</sub>) was lower than that of base alloy at all oxidation temperatures.
- 3-The Y<sub>2</sub>O<sub>3</sub> and Nd<sub>2</sub>O<sub>3</sub> particles dispersion in matrix of the base alloy (Al-Li) improve the oxidation resistance of this alloy at high temperatures ( 500°C and 550°C ).
- 4-The presence of RE oxides in the base alloy (Al-Li) decreases the growth rate of Li<sub>2</sub>O and Li<sub>2</sub>CO<sub>3</sub> scales.
- 5-The Y<sub>2</sub>O<sub>3</sub> and Nd<sub>2</sub>O<sub>3</sub> particles improve the adherence of protective oxide even after extended periods of oxidation.
- 6-The RE atoms block Li-atoms diffusion along grain boundaries and consequently the Li-oxides on RE oxide containing specimens are considerably thinner.
- 7- X-ray diffraction analysis of the oxide scale of specimens shows the presence of Y<sub>2</sub>O<sub>3</sub> and Nd<sub>2</sub>O<sub>3</sub> particles in external scale and uniformly distributed in matrix of base alloy.

#### 5. References:

1. Martin J. "Aluminum Lithium Alloys", Ann. Rev. Mat. Sci., Vol.18, 1989, PP.101-119.
2. Jaroslaw Mizera , Malgarzata Lewandowskq , Alexander V. korzikov , Krzysztof J. and Kurzydowski, "Microstructure and Mechanical Properties of Binary AL-Li Alloys Processed by ECAE" ,Solid State Phenomena ,Vols.101-102 , 2005, PP.73-76.
3. Brue M .and Papazian J.M., "Elevated Temperature Oxidation of Al-Li Alloy", 3rd Int. Al-Li Conf. London,1986, PP.287-293.
4. Partridge P.G., "Oxidation of Al-Li Alloy in the Solid State", International Materials Reviews, Vol.35, No.1, 1990, PP.37-60.
5. Son k .k .Williams J.M., Chabalo J.M., Levi – Setti R. and Newbury D.C., "Role of Second Phase Particles in The Oxidation of Al-Li Alloys" , Oxid. Met., Vol.37, No.2 , 1992, PP.23-37.
6. Polymer I.J., "Light Alloys", Metallurgy of The Light Metal, 2nd Ed., Edward Arnold, A division of Hodder & Stoughton, 1989.
7. Barki A.W, Al-Haidary J.T. and Rozoki R.N., Eng.and Techn. J. Vol.11, No.8, 1992 , P72.
8. Al-Haidary J.T and Abbass M.K., "Effect of Ge ,Te and Y Additions on Oxidation and Properties of Al-Li alloy", Dirasat Journal Eng. Sci , No.1, 2000, Muharram University of Jordan ,PP.153-169.
9. Pint B.A., More K. L, Tortorelli P.F., Porter W.D. and Wright I.G. ,"Optimizing The Imperfect Oxidation Performance of Iron

- Alumindes” ,Oak Ridge National Laboratory ,USA ,2003,www.Internet.
10. Fernandes S.M.C. and Romanathan L.V.,” Rare Earth Oxide Coating to Decrease High Temperature Degradation of Chromia Forming Alloys” , Materials Research ,Vol.7, No.1, 2004, PP.1-5.
  11. Giggins C.B.and Pettit F.S., ”The Oxidation of TDNiC (Ni-20Cr-2Vol pct ThO<sub>2</sub>) Between 900C°and 1200C° ”, Metallurgical Transaction ,Vol.4 ,1971, PP.1071-1078.
  12. Muna K.Abbas, Ph.D.Thesis, “Effect of Trace Additions of Alloying Elements on Oxidation and Some Properties of Base Al-Li Alloy”, University of Technology, Baghdad –Iraq, 1995.
  13. Delaunay D .and Huntz A.M. ,”Mechanisms of Adherence of Alumina Scale Developed During High Temperature Oxidation of Fe-Ni-Cr-Al-Y Alloys” , Journal of Mat. Sci., Vol.17, 1982, P2077.
  14. Chevalier G., Bonnet J.G., Dufour P. and Larpin J.P., “ The REE: Away to Improve The High Temperature Behavior of Stainless Steels ?”, Surface and Coatings Technology” ,Vol.100-101,1998, PP.208-223.
  15. Papaicovou P. and Hussey R.J., Corrosion Sci., Vol.30, No.4/5,1990, P451 .
  16. Denny A. Jones, “Principles and Prevention of Corrosion”, 2nd Ed., Prentice Hall, Upper Saddle River, 1996.
  17. Khalil Al-Hatab, “Effect of Environment on Oxidation Behavior of Inconel Alloy 600 ,Ph.D. Thesis, University of Technology ,Baghdad –Iraq ,2004
  18. Panter J., Viguer J. and Andrieu E.,” Microstructural Evolution of Alloy 600 during Dry Oxidation”, Materials Science Forum, Vols.369-372, 2001, PP.141-148.





**Alloy C**

**Figure (1)** Microstructure of the prepared alloys after casting , deformation and solution heat treatment

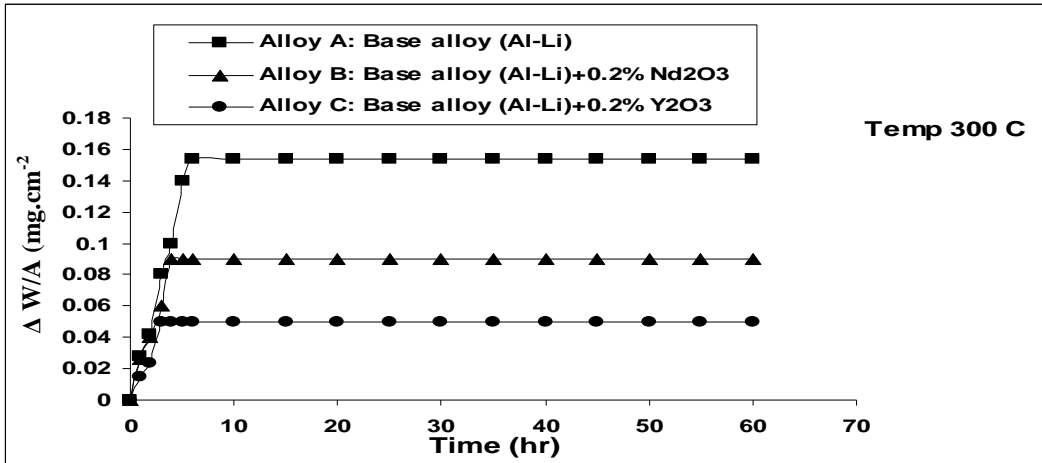


**Figure (2)** Weight gain/ unit area with time for oxidation of the alloys(A,B,C) at 300°C

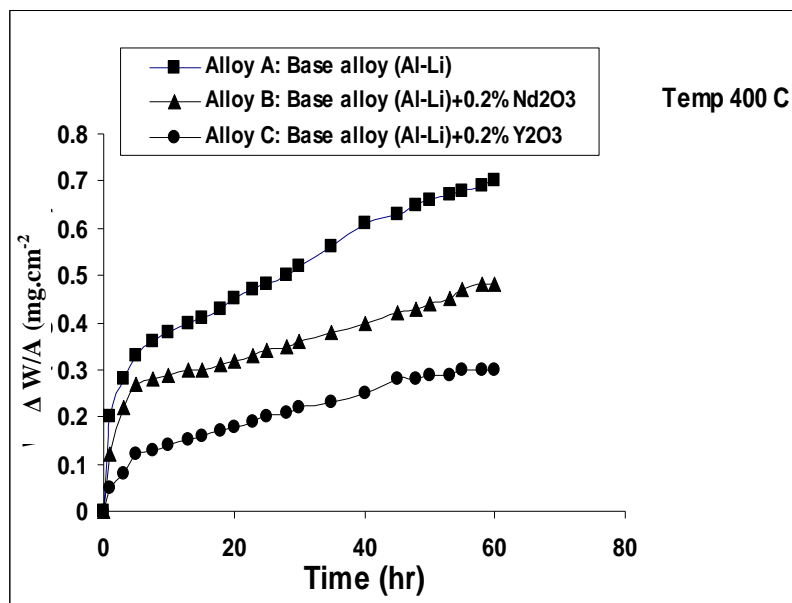


Figure (3) Weight oxidation of the alloys gain/ unit area with time for (A,B,C) at 400°C

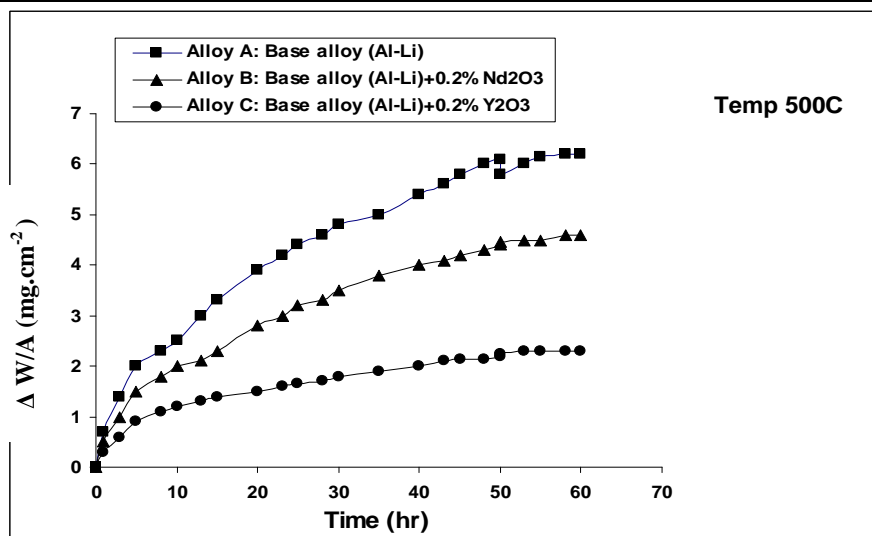


Figure (4) Weight gain/ unit area with time for oxidation of the alloys(A,B,C) at 500°C



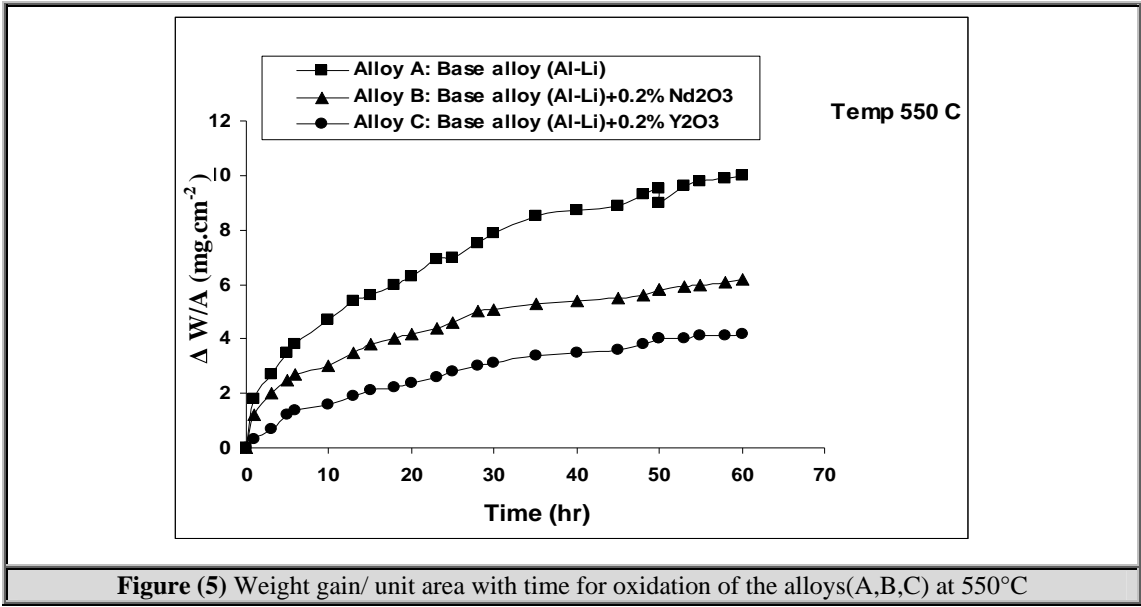


Figure (5) Weight gain/ unit area with time for oxidation of the alloys(A,B,C) at 550°C

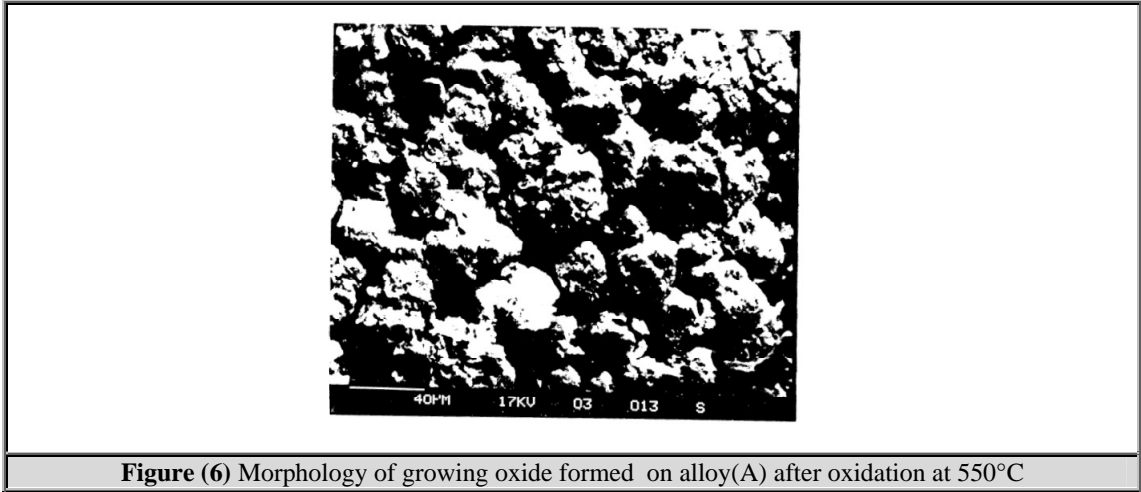


Figure (6) Morphology of growing oxide formed on alloy(A) after oxidation at 550°C

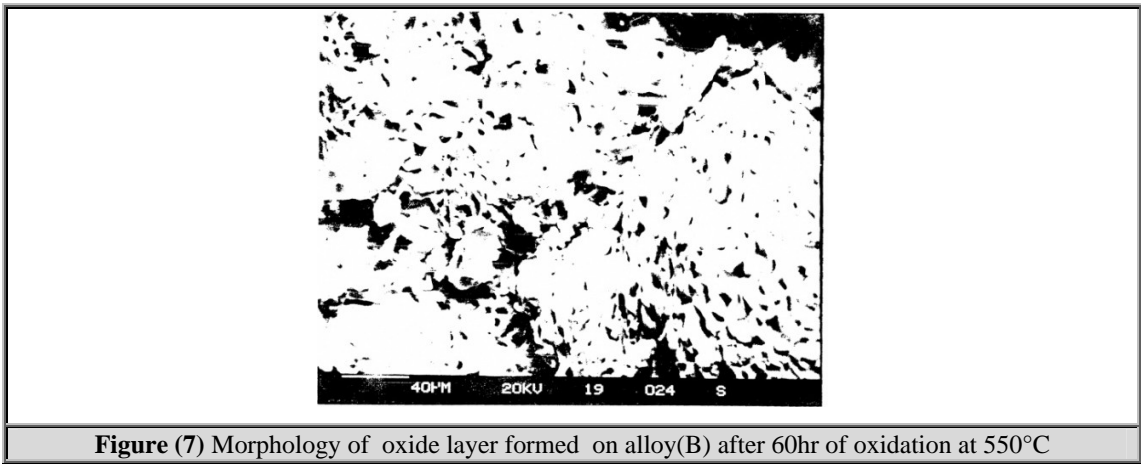
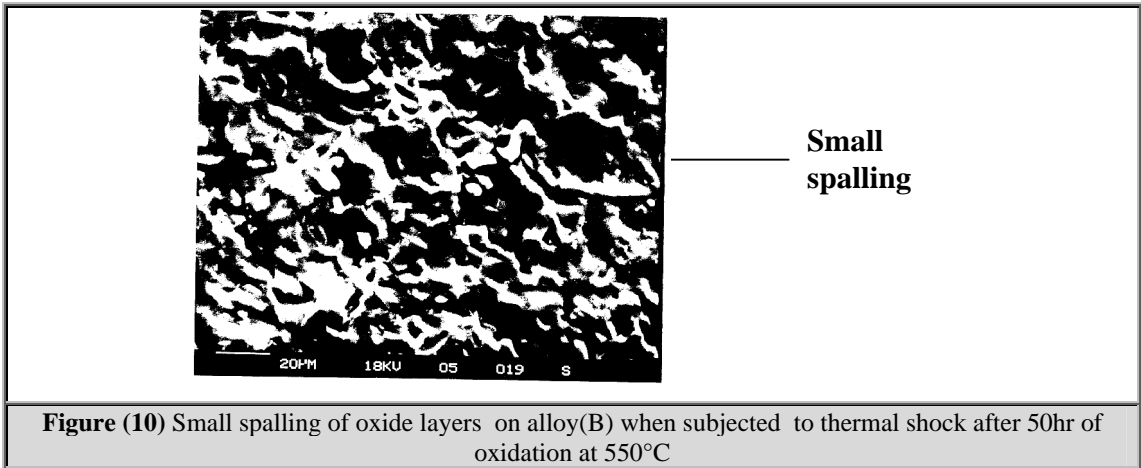
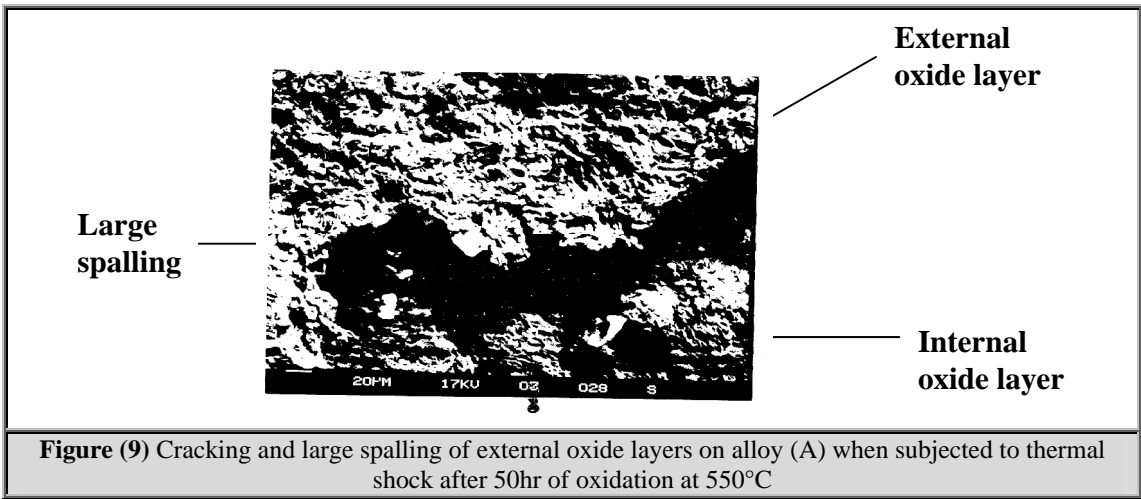
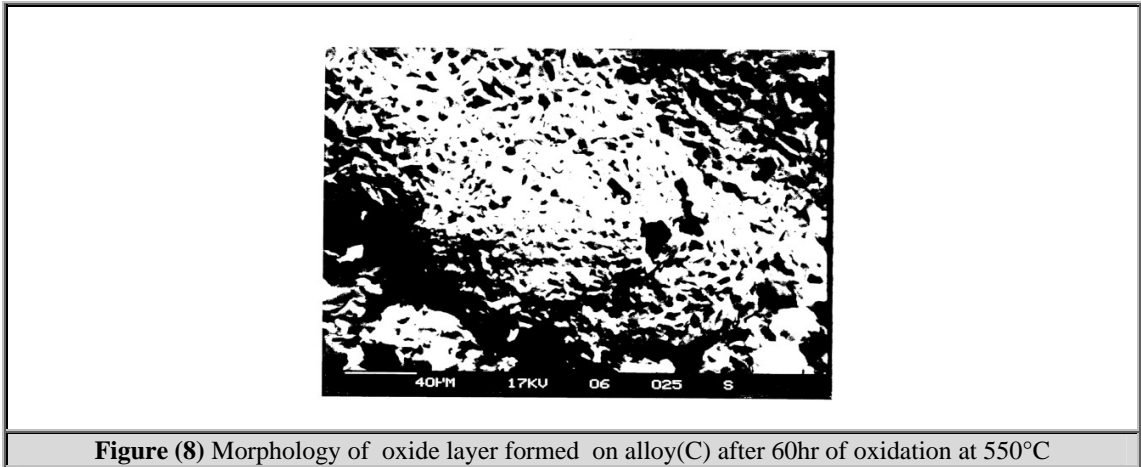
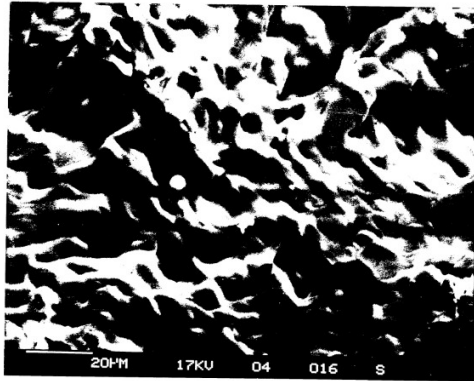
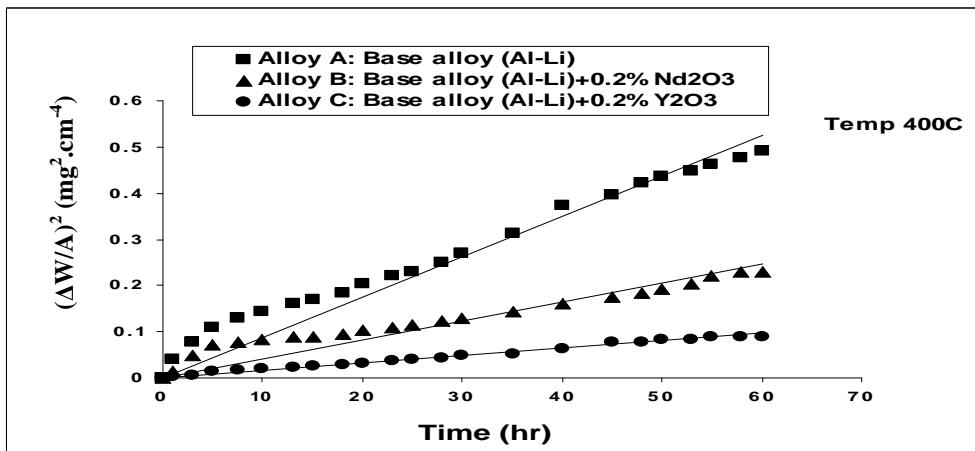


Figure (7) Morphology of oxide layer formed on alloy(B) after 60hr of oxidation at 550°C





**Figure (11)** Growing oxide layers on alloy(C) remains sound and intact when subjected to thermal shock after 50hr of oxidation at 550°C



**Figure (12)** Square of the weight gain/ unit area vs time for alloys(A, B and C ) oxidized at temperature 400°C for up to 60hrs

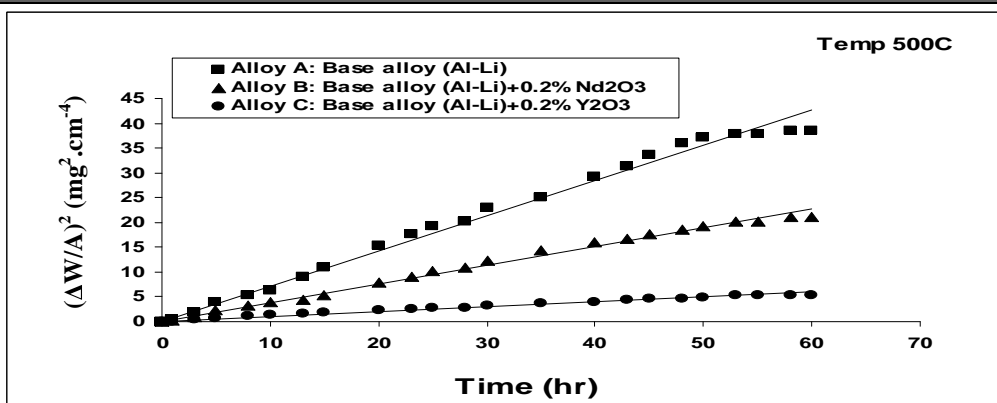


**Figure (13)** Square of the weight gain/ unit area vs time for alloys(A, B and C ) oxidized at temperature 500°C for up to 60hrs

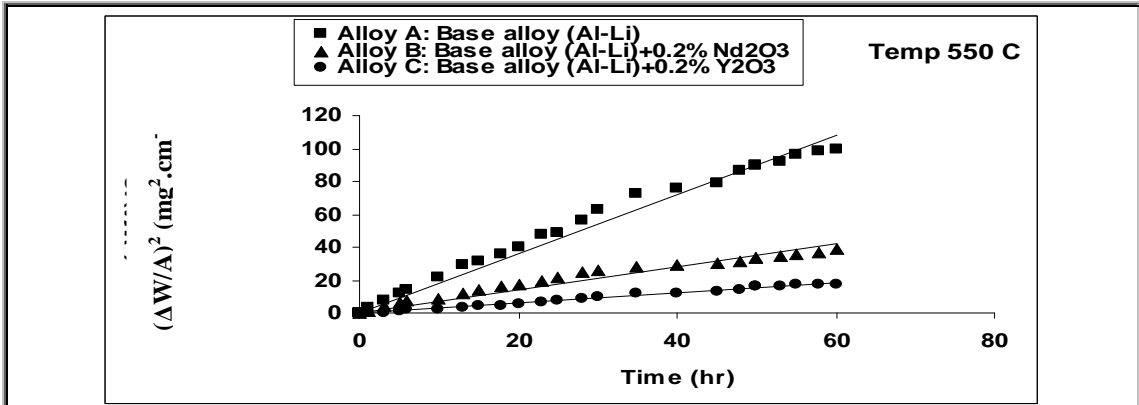


Figure (14) Square of the weight gain/ unit area vs time for alloys(A, B and C ) oxidized at temperature 550°C for up to 60hrs

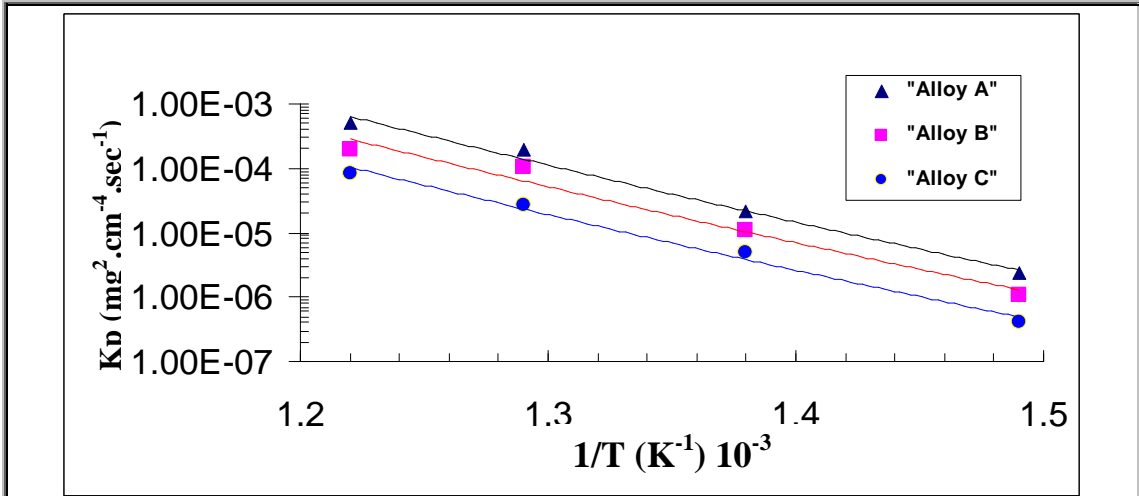


Figure (15) parabolic rate constants for the oxidation of alloys (A, B and C) as a function of temperature for up to 60 hrs in dry air

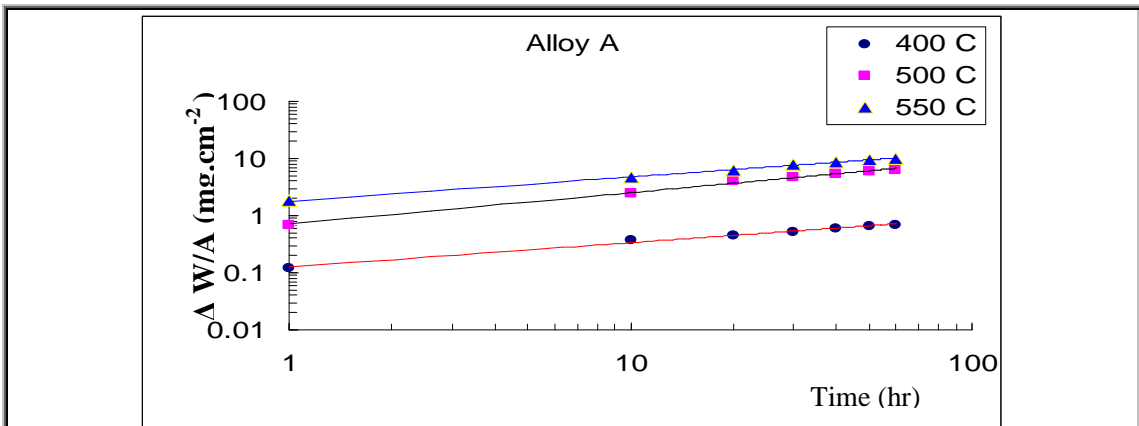


Figure (16) Typical log-log plots of oxidation weight gain data for alloy (A) at temperatures range 400°C-550°C for up to 60hr in dry air

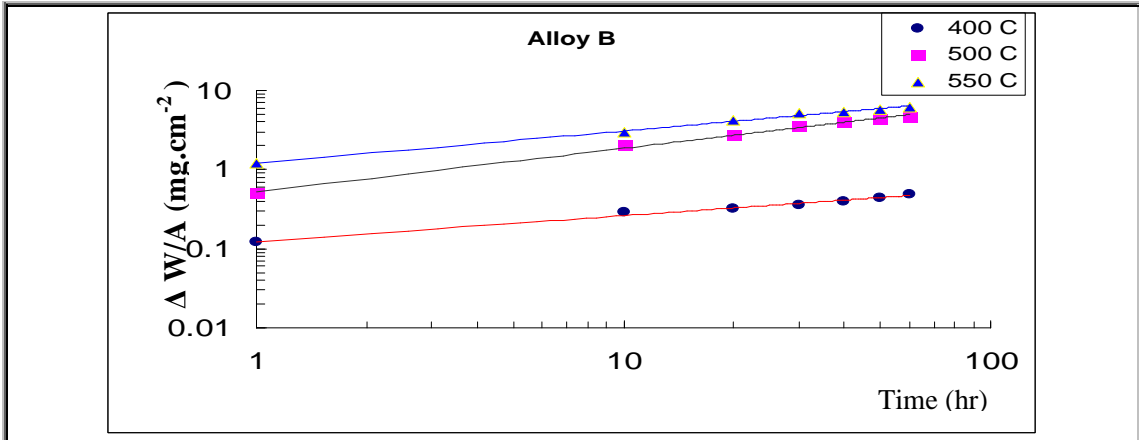


Figure (17) Typical log-log plots of oxidation weight gain data for alloy (B) at temperatures range 400°C-550°C for up to 60hr in dry air

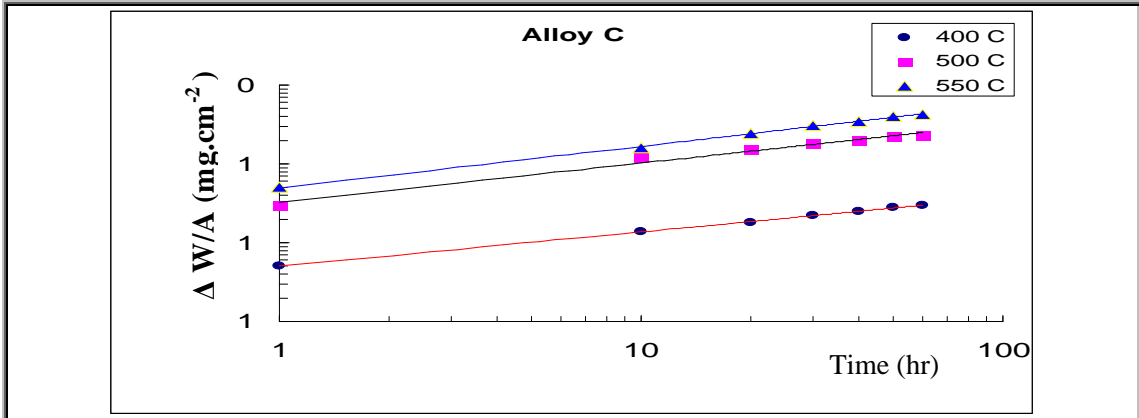
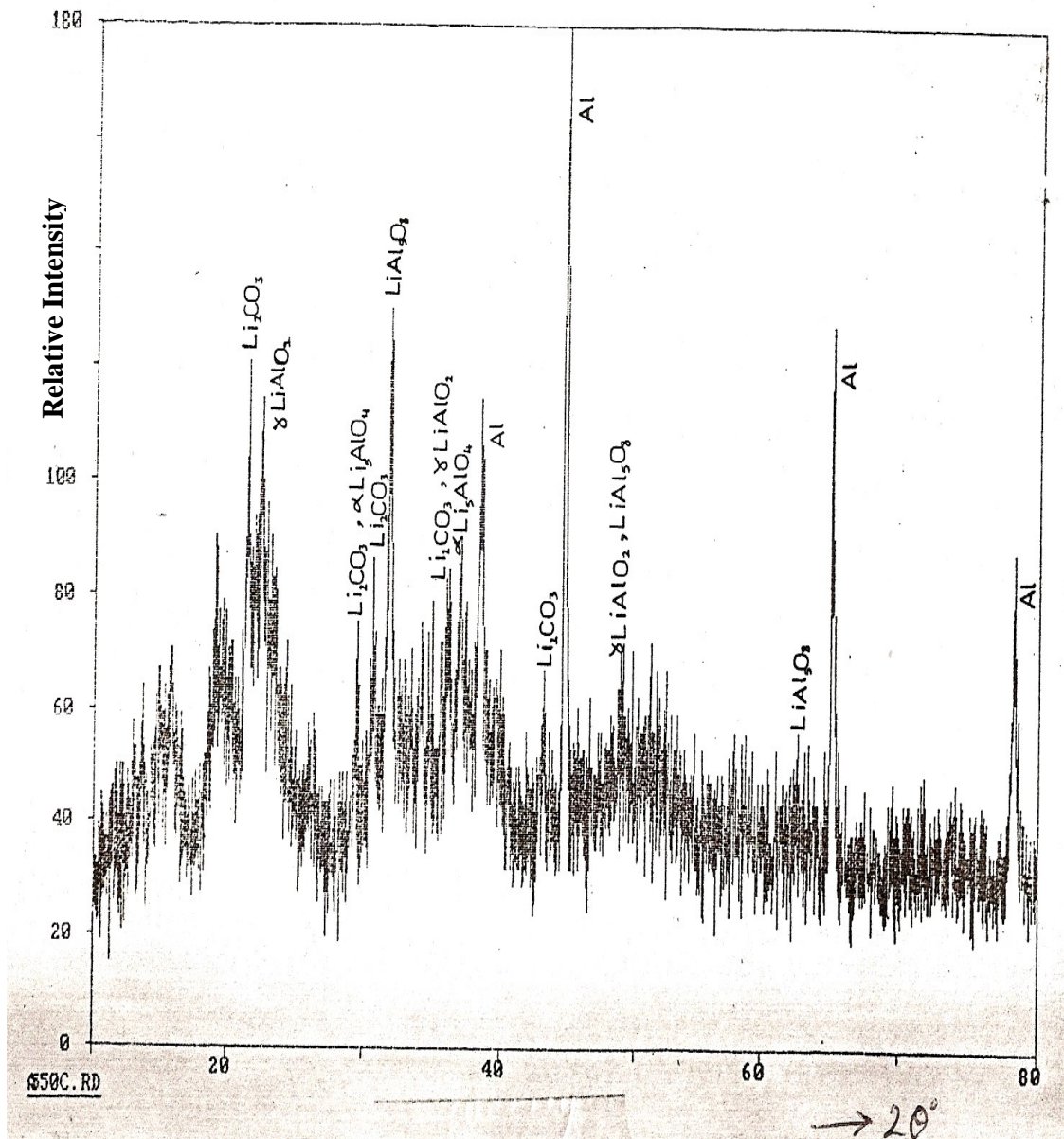
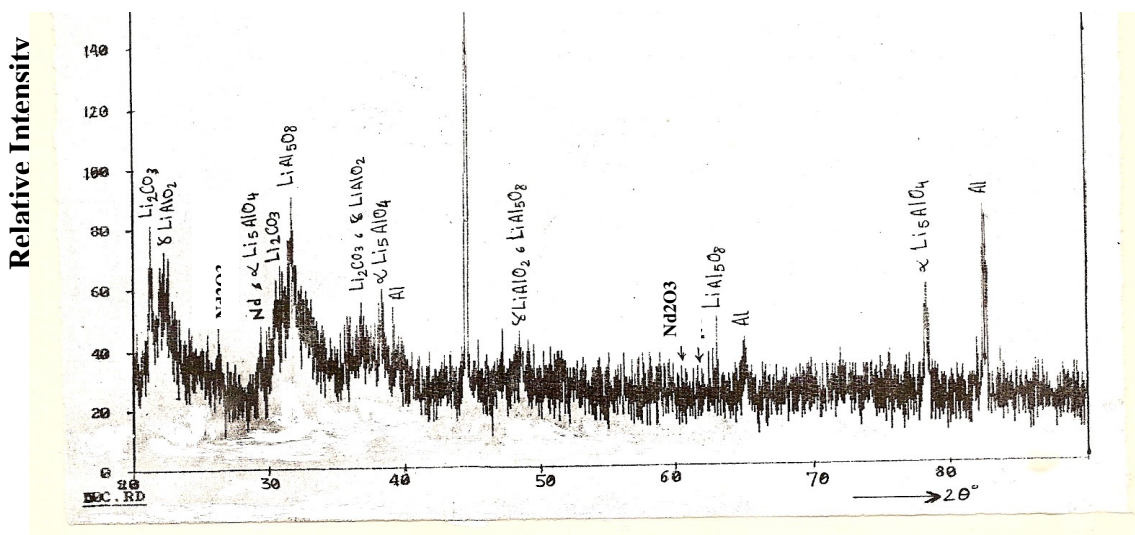


Figure (18) Typical log-log plots of oxidation weight gain data for alloy (C) at temperatures range 400°C-550°C for up to 60hr in dry air



Appendix A : x-ray diffraction analysis of alloy A



Appendix B : x-ray diffraction analysis of alloy B

# تأثير اكاسيد العناصر النادرة ( $Y_2O_3$ و $Nd_2O_3$ ) على السلوك الكيناتيكي للتأكسد لسبيكة المنيوم-ليثيوم

د.منى خضير عباس ( أستاذ مساعد )  
قسم هندسة الإنتاج والمعادن/ الجامعة التكنولوجية

## الخلاصة

تم دراسة التأكسد لسبيكة أساس ( المنيوم- ليثيوم ) تحتوي على كميات قليلة من دقائق الاوكسيدية من العناصر النادرة (  $Y_2O_3$  و  $Nd_2O_3$  ) في درجات حرارية (  $300^{\circ}C - 550^{\circ}C$  ). وتم تحضير هذه السبائك بعملية الصهر والصب في قوالب فولاذية وتحت أجواء مسيطر عليها. أن عنصر الليثيوم يتأكسد انتقائيا مكونا مجموعة من الأكاسيد  $Li_2O$  ,  $LiAl_5O_8$  ,  $Li_2CO_3$  و  $Li_5AlO_4$  وكانت قيم ثابت معدل التأكسد القطع المكافئ ( $K_p$ ) للسبيكة الاساس أعلى مما في حالة السبائك الاخرى الحاوية على أكاسيد  $Y_2O_3$  و  $Nd_2O_3$  تحت ظروف مماثلة. وجد ان السبيكة الحاوية على دقائق الليثيوم (  $0.2\% Y_2O_3$  ) تمتلك أقل معدل تأكسد اي اعلى مقاومة تأكسد مقارنة مع السبائك الاخرى. وكذلك وجد ان الاكاسيد المتكونة على السبيكة الاساس (  $Al-Li$  ) تتعرض الى التشقق والتفشر عند اجراء الصدمة الحرارية في درجة حرارة  $500^{\circ}C$  و  $550^{\circ}C$  بعد مرور 50 ساعة من التأكسد. تم التعرف على السلوك الكيناتيكي العام للتأكسد بأجراء قياسات الوزن المكتسب للسبائك عند التأكسد الايزوثيرمي في الهواء الجاف وكذلك اجراء فحص حيود الاشعة السينية. وأستخدم المجهر الالكتروني الماسح لدراسة طوبوغرافية وبنية الطبقات الاوكسيدية المتكونة على السطح، وقد أظهرت نتائج التأكسد ان كل السبائك تخضع لقانون القطع المكافئ في جميع الدرجات الحرارية المستخدمة في البحث ما عدا الدرجة الحرارية  $300^{\circ}C$  حيث تخضع تقريبا للقانون اللوغارتمي.



This document was created with Win2PDF available at <http://www.daneprairie.com>.  
The unregistered version of Win2PDF is for evaluation or non-commercial use only.